Geometric Parameters Optimization of Cable-Driven Parallel Robot with a Movable Gripper

Elena V. Gaponenko, Dmitry I. Malyshev, Victoria S. Kuzmina, and Larisa A. Rybak

Abstract The chapter considers the structure of a cable-driven parallel robot for load move in special conditions. This structure is a rigidly fixed frame connected by tensioned ropes to a platform containing an axial movement device. Effective numerical methods and algorithms were developed and tested, which allowed investigating the influence of cable pulling forces on the volume of the operating area and determine the minimum geometric dimensions of the robot that ensure the movement of the output link within the required operating area. In order to implement the proposed methods and algorithms, a software package with the ability to export 3D operating areas in STL format for visualization was developed. The chapter presents the results of mathematical modeling.

Keywords cable-driven parallel robot · Interval analysis · Tensile forces · Algorithm · Geometric parameters

1 Introduction

In recent decades, there has been a growing demand for the use and control of manipulators in various industrial sectors in order to increase productivity, reliability, accuracy, rigidity, and access to the setting inaccessible to humans. Cable-driven parallel robots (CDPR) are of particular interest. They present a special type of kinematic structure, consisting mainly of a work tool connected to a fixed base platform using cables [1–3]. Today, cable robots are successfully used for construction work [4], for measuring the position and orientation of an object [5, 6], for rehabilitation in medicine [7–9], as well as for solving other industrial problems [10]. CDPRs use cables instead of pull-out rods to control the position of the output link. In these mechanisms, the position of the output link is controlled by changing the length of the cables. Cables are usually wound on spools attached to a base and powered by a rotating motor.

E. V. Gaponenko (✉) · D. I. Malyshev · V. S. Kuzmina · L. A. Rybak
Belgorod State Technological University named after V.G. Shukhov, 46 Kostukova, Belgorod 308012, Russia
e-mail: gaponenkobel@gmail.com

A. G. Kravets et al. (eds.), *Cyber-Physical Systems: Design and Application for Industry 4.0*, Studies in Systems, Decision and Control 342,
https://doi.org/10.1007/978-3-030-66081-9_5

CDPRs have such advantages as a large workspace, assembly and disassembly ease, high mobility, heavy load capacity and reset ease. Controlling the length of the cables over a wide range, we can get access to a very large workspace from several tens of centimeters to several tens of meters or more. The use of cables instead of rigid links further reduces weight since the drills do not change position and are fixed to a stable base so that the only moving parts are the cables and the output link. As a result, a robot with higher speed and maneuverability and in-creased heavy load is obtained. The production costs of CDPRs are significantly lower than those of conventional manipulators. CDPRs are easy to install. Such a manipulator can be assembled using a number of inexpensive winches and cables. In addition, since the motors do not need to be installed close to a moving platform, they are suitable for use in hazardous environments. In addition, their heavy load capacity is relatively high; it is even comparable to construction cranes.

The following authors pay particular attention to the topic of CDPRs: J. B. Isard, M. Michelin, J. P. Merle, K. Gosselin, S. Baradat, and others. Bouchard and Gossla were engaged in the optimization of the workspace of a CDPR for broadcasting. Thus, in the paper [11], some issues related to inverse kinematics and statics of CDPRs are considered, as well as some limitations typical of workspace. Abbasneyad and the research team developed a planar CDPR for rehabilitation purposes and balancing external forces. J. P. Merle and D. Denis developed the lightweight and mobile cable parallel robot Marionet, which is designed for rescue operations in hard-to-reach places. The article [12] considers the dynamic planning of the 3-DOF trajectory of spatial suspended parallel manipulators. On the basis of the dynamic model of the suspended robot, a set of algebraic inequalities representing the constraints on the cable tension is obtained. During the use of periodic functions in the design of trajectories, it is shown that there are special frequencies, similar to the natural frequencies of pendulum-type systems. These special frequencies can be used in practice to simplify trajectory planning. A prototype of a 3-DOF CDPR was developed in [13]. The proposed approach to trajectory planning can be used to plan dynamic trajectories that go beyond the static workspace of the mechanism, giving new applications and opportunities for CDPRs. The paper [14] considers the dynamic analysis and classification of the workspace based on the general equation of motion of the CDPR and the one-sided properties of cables. Different types of workspaces were qualitatively compared. Zhang and Shang [15] were engaged in planning the trajectory of a three-stage cable robot taking into account dynamic effects. In their work, a geometric approach for trajectory planning was proposed, which can also be applied when the mechanism goes beyond the static equilibrium. The approach proposed by the authors provides an analytical solution that allows for positive and continuous tensions in all control cables. The influence of dynamic behavior of control cables was shown by Du et al. [16], where the authors used a dynamic cable model with variable length to control a mobile platform.

One of the main tasks in CDPR designing is workspace determination, within which the operating body should be located during the technological operations. In order to determine the workspace, the following methods are used: geometric, numerical, discretization methods. One of the existing deterministic methods is the

non-uniform covering method. The cover set is represented by a set of n-dimensional boxes, the boundaries of which are described as:

$$\underline{x_i} \leq x_i \leq \overline{x_i}, i \in 1, n \tag{1}$$

This method can be easily automated and applied to various tasks, including in the field of robotics. The non-uniform covering method used to determine the workspace of some types of parallel robots is considered in [17–19].

The use of the method of non-uniform covering to determine the workspace of a CDPR designed to application in special conditions was discussed earlier in the work [20]. Within the framework of this chapter, we will determine the minimum geometric parameters of a CDPR depending on the required dimensions of the workspace for the performance of technological operations. In addition, we will investigate the influence of cable tension forces on the volume of the workspace for two configurations: with and without axial movement of the output link.

2 Mathematical Model

Let us consider the structure of a CDPR designed for application in special conditions (Fig. 1). The mechanism consists of four columns, four cables, which are connected with one of the ends to the movable platform at points B_1, B_2, B_3, B_4. The gripping unit with the possibility of axial movement is fixed on the platform. The second ends of the cables passed through the pulleys, designated by points A_1, A_2, A_3, A_4, installed on the columns, they are fixed on the drums D_1, D_2, D_3, D_4, respectively. Under the action of the load weight mg, fixed at point C, tensile forces T_1, T_2, T_3, T_4 appear in the cables. The change in the position of the load-attaching point occurs due to the change in the lengths of the cables when the drums rotate with the gear motors M_1, M_2, M_3, M_4. The gripping unit is a movable platform connected with cables. An output link C is located on the movable platform, which has the ability to axially move h along the Z axis. This mechanism allows objects to be moved in hard-to-reach places with special conditions without human intervention, for example, the

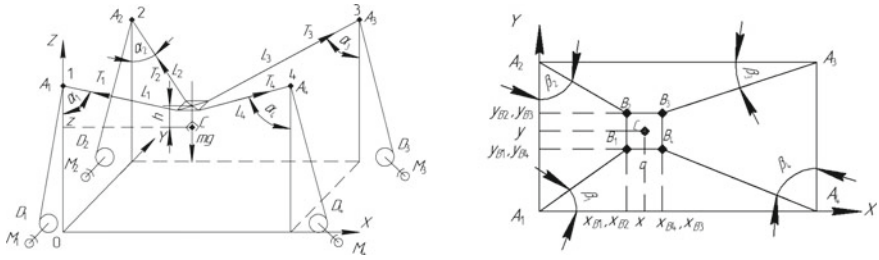

Fig. 1 Cable-driven parallel robot

work with radioactive elements and radiation sources, the work with elements that can irradiate cells, lead to their mutation. They can cause irreparable harm to health. This category also includes work at nuclear, thermal power plants.

Despite many advantages of CDPRs, there are several problems associated with the control of the movement of robot cables. One of the disadvantages is that cables can be pulled but not pushed, resulting in a one-way restriction whereby the cables must always be kept tensed. The positions in which at least one of the cables is loose are special and are not considered in the chapter.

We introduce the limits on the cable tensile forces T_i:

$$T_{\mathbf{i}} := \left[\underline{T_{\mathbf{i}}}, \overline{T_{\mathbf{i}}}\right] = \{0 \le \underline{T_i} \le T_i \le \overline{T_{\mathbf{i}}}\}, \tag{2}$$

Let us write down the intervals that describe the ranges of the cosines and sines of the angles αi and βi:

$$S_{\mathbf{Ai}} := \left[\underline{S_{\mathbf{Ai}}}, \overline{S_{\mathbf{Ai}}}\right] = \left\{\underline{S_{\mathbf{Ai}}} \le \sin\alpha_i \le \overline{S_{\mathbf{Ai}}}\right\}, i \in 1, \ldots, 4,$$

$$S_{\mathbf{Bi}} := \left[\underline{S_{\mathbf{Bi}}}, \overline{S_{\mathbf{Bi}}}\right] = \{S_{\mathbf{Bi}} \le \sin\beta_i \le \overline{S_{\mathbf{Bi}}}\}, i \in 1, \ldots, 4,$$

$$\mathbf{C_{Ai}} := \left[\underline{\mathbf{C_{Ai}}}, \overline{\mathbf{C_{Ai}}}\right] = \left\{\underline{\mathbf{C_{Ai}}} \le \cos\alpha_i \le \overline{\mathbf{C_{Ai}}}\right\}, i \in 1, \ldots, 4,$$

$$\mathbf{C_{Bi}} := \left[\underline{\mathbf{C_{Bi}}}, \overline{\mathbf{C_{Bi}}}\right] = \left\{\underline{\mathbf{C_{Bi}}} \le \cos\beta_i \le \overline{\mathbf{C_{Bi}}}\right\}, i \in 1, \ldots, 4.$$

The tensile forces in flexible links can be calculated by solving systems of nonlinear equations of the form:

$$\begin{cases} T_1 S_{A1} C_{B1} + T_2 S_{A2} S_{B2} - T_3 S_{A3} C_{B3} - T_4 S_{A4} S_{B4} = 0 \\ T_1 S_{A1} S_{B1} - T_2 S_{A2} T_{B2} - T_3 S_{A3} S_{B3} + T_4 S_{A4} C_{B4} = 0 \\ T_1 C_{A1} + T_2 C_{A2} + T_3 C_{A3} + T_4 C_{A4} - mg = 0 \end{cases} \tag{3}$$

where $\mathbf{C_{Ai}} = \frac{z_{Ai} - \mathbf{Z_{Bi}}}{\sqrt{(\mathbf{X_{Bi}} - x_{Ai})^2 + (\mathbf{Y_{Bi}} - y_{Ai})^2 + (z_{Ai} - \mathbf{Z_{Bi}})^2}}$, $\mathbf{S_{Ai}} = \frac{\sqrt{(\mathbf{X_{Bi}} - x_{Ai})^2 + (\mathbf{Y_{Bi}} - y_{Ai})^2}}{\sqrt{(\mathbf{X_{Bi}} - x_{Ai})^2 + (\mathbf{Y_{Bi}} - y_{Ai})^2 + (z_{Ai} - \mathbf{Z_{Bi}})^2}}$; $\mathbf{S_{B1}} = \frac{\mathbf{Y_{B1}} - y_{A1}}{\sqrt{(\mathbf{X_{B1}} - x_{A1})^2 + (\mathbf{Y_{B1}} - y_{A1})^2}}$; $\mathbf{S_{B2}} = \frac{\mathbf{X_{B2}} - x_{A2}}{\sqrt{(\mathbf{X_{B2}} - x_{A2})^2 + (y_{A2} - \mathbf{Y_{B2}})^2}}$; $\mathbf{S_{B3}} = \frac{y_{A3} - \mathbf{Y_{B3}}}{\sqrt{(x_{A3} - \mathbf{X_{B3}})^2 + (y_{A3} - \mathbf{Y_{B3}})^2}}$; $\mathbf{S_{B4}} = \frac{x_{A4} - \mathbf{X_{B4}}}{\sqrt{(x_{A4} - \mathbf{X_{B4}})^2 + (\mathbf{Y_{B4}} - y_{A4})^2}}$; $\mathbf{C_{B1}} = \frac{\mathbf{X_{B1}} - x_{A1}}{\sqrt{(\mathbf{X_{B1}} - x_{A1})^2 + (\mathbf{Y_{B1}} - y_{A1})^2}}$; $\mathbf{C_{B2}} = \frac{y_{A2} - \mathbf{Y_{B2}}}{\sqrt{(\mathbf{X_{B2}} - x_{A2})^2 + (y_{A2} - \mathbf{Y_{B2}})^2}}$; $\mathbf{C_{B3}} = \frac{x_{A3} - \mathbf{X_{B3}}}{\sqrt{(x_{A3} - \mathbf{X_{B3}})^2 + (y_{A3} - \mathbf{Y_{B3}})^2}}$; $\mathbf{C_{B4}} = \frac{\mathbf{Y_{B4}} - y_{A4}}{\sqrt{(x_{A4} - \mathbf{X_{B4}})^2 + (\mathbf{Y_{B4}} - y_{A4})^2}}$.

with $\mathbf{X_{B1}} = \mathbf{X_{B2}} = \mathbf{X_C} - \frac{a}{2}$, $\mathbf{X_{B3}} = \mathbf{X_{B4}} = \mathbf{X_C} + \frac{a}{2}$, $\mathbf{Y_{B1}} = \mathbf{Y_{B4}} = \mathbf{Y_C} - \frac{a}{2}$, $\mathbf{Y_{B2}} = \mathbf{Y_{B3}} = \mathbf{Y_C} + \frac{a}{2}$, $\mathbf{Z_{Bi}} = \mathbf{Z_C} + \mathbf{H}$,где $\mathbf{X_C} := \left[\underline{\mathbf{X_C}}, \overline{\mathbf{X_C}}\right] = \left\{\underline{\mathbf{X_C}} \le x_c \le \overline{\mathbf{X_c}}\right\}$, $\mathbf{Y_C} := \left[\underline{\mathbf{Y_C}}, \overline{\mathbf{Y_C}}\right] = \left\{\underline{\mathbf{Y_C}} \le y_c \le \overline{\mathbf{Y_c}}\right\}$, $\mathbf{Z_C} := \left[\underline{\mathbf{Z_C}}, \overline{\mathbf{Z_C}}\right] = \left\{\underline{\mathbf{Z_C}} \le z_c \le \overline{\mathbf{Z_c}}\right\}$, $\mathbf{H} := \left[\underline{\mathbf{H}}, \overline{\mathbf{H}}\right] = \left\{\underline{\mathbf{H}} \le h \le \overline{\mathbf{H}}\right\}$.

The left parts of the system of Eqs. (2) are the functions in the form g_j, $j \in 1, ..., 3$: $g_1 = T_i S_{A1} C_{B1} + T_2 S_{A2} S_{B2} - T_3 S_{A3} C_{B3} - T_4 S_{A4} S_{B4}, \ldots, g_3 = T_1 C_{A1} + T_2 C_{A2} + T_3 C_{A3} + T_4 C_{A4} - mg$.

The above-mentioned equations allow finding solutions to the system of Eqs. (2) that determine the limitations of the workspace.

3 Analysis of the Effect of Cable Tension Forces.

The approximation algorithm of the set of solutions to systems of nonlinear inequalities for the determination of the workspace is considered in the work [20]. Let us analyze the influence of the cable tensile force ranges on the basis of the obtained algorithm.

We introduce the coefficient k, which is defined as $k = \overline{T_i} / \underline{T_i}$. Let us define the workspace for different values of k in the range from 1, 4 to 10 with an interval 0,1. Let us take the minimum tensile force $\underline{T_i} = 10$ H.

The computational experiment was carried out for the following parameters of the mechanism: $x_{A3} = x_{A4} = y_{A2} = x_{A2} = z_{Ai} = 1000$ mm, $m = 5$ kg.

Two configurations of the cable mechanism were considered: without axial movement of the output link and with movement h = 100 mm. The algorithm is implemented in the C++ programming language using the Snowgoose interval analysis library [21], as well as the OpenMP library for the implementation of multi-threaded calculations [18]. The computation time for $k = 5$ without axial movement, approximation accuracy of 4 mm, and using the parallelization of calculations for 8 threads on a personal computer was 3 min. 46 s.

The dependence of the volume of the workspace on the coefficient k is shown in Fig. 2. As can be seen from the figure, the volume of the workspace for the configuration with axial movement of the output link is greater for any k, however, at $k \geq 9.5$ the volume of the workspace is almost equal.

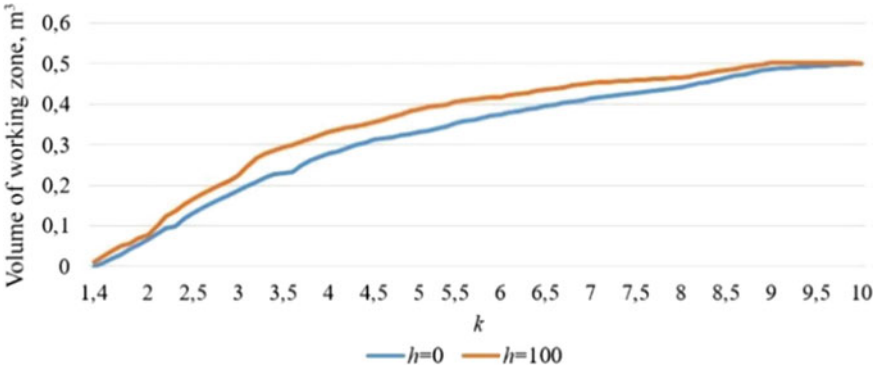

Fig. 2 Volume change of the workspace depending on the coefficient k

In order to evaluate the change in the form of the workspace, the output of the simulation results in STL format was used. Figure 3 shows the workspaces at $k = 3$ (green) and $k = 8$ (blue). Figure 4 shows the change in the workspace at $k = 3$ without axial movement of the output link (green) and with axial movement (blue).

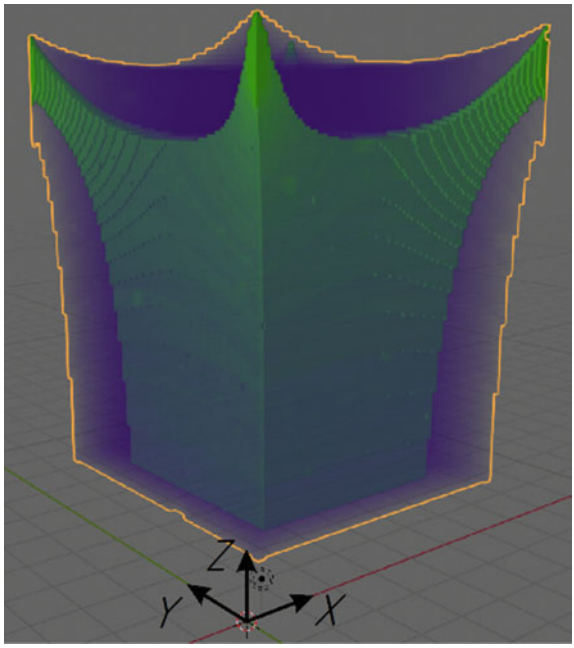

Fig. 3 Workspace at different k values

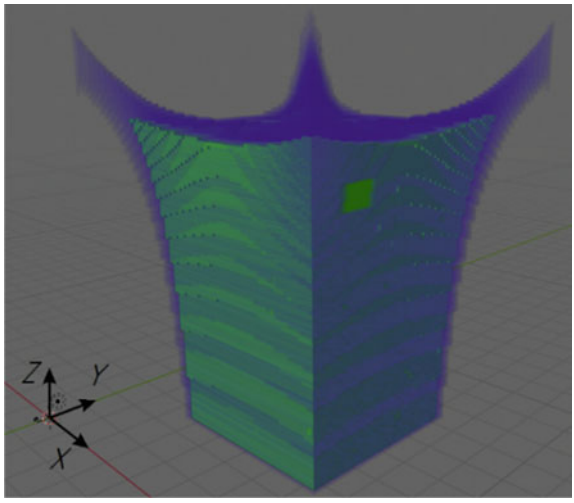

Fig. 4 Increase of workspace due to the axial movement of the output link

4 Geometric Parameters Optimization

Next, we will analyze the optimization of the geometric parameters of the cable mechanism. It includes the selection of the minimum overall dimensions of the CDPR, providing the required dimensions of the workspace. For this, using the methods of interval analysis, we will check whether the system can be solved (3).

In this case, the coordinates correspond to the coordinates of the boundaries' points of the required workspace, the coordinates lie in the interval, the length of which depends on the range of possible location of the required workspace inside the robot along the *Z*-axis. We synthesize an algorithm for the optimization of geometric parameters using a system of equations written in the general form:

$$\begin{cases} g_i(x) = 0, \\ \cdots \\ g_m(x) = 0, \\ a_i \le x_i \le b_i, i = 1, \ldots, n. \end{cases} \tag{4}$$

The algorithm (Fig. 5) works with two lists of six-dimensional boxes $\mathbb{P}$ (current list), $\mathbb{P}_A$ (cover). Each of the dimensions of the boxes corresponds to the intervals $T_\mathbf{i}$, $i = 1, \ldots, 4$, $\mathbf{Z}_c^{'}$ и H.

The initial box Q, which covers the entire set of solutions X, is determined by the interval limits $a_i \le x_i \le b_i, i = 1, \ldots, n$. Let us consider any box B. Let $m(B) = \max\limits_{j=1,\ldots,m} \min\limits_{x \in B} g_j(x)$ and $M(B) = \max\limits_{j=1,\ldots,m} \max\limits_{x \in B} g_j(x)$. If $m(B) > 0$ or $M(B) < 0$, then contains no possible points for system (4). Initially, the overall dimensions of the robot are equal to the dimensions of the required workspace, that is $x_{A3} = x_{\max}^{(w)}$, $y_{A3} = y_{\max}^{(w)}$, $z_{A3} = z_{\max}^{(w)}$.

The algorithm works as follows:

1. To set geometric parameters of the required workspace, intervals H, $T_\mathbf{i}$,$i \in 1, \ldots,$ 4. and approximation accuracy δ.
2. To assign $x_{A3} = x_{\max}^{(w)}$, $y_{A3} = y_{\max}^{(w)}$, $z_{A3} = z_{\max}^{(w)}$.
3. The list $\mathbb{P}_A$ is empty, the l sit $\mathbb{P}$ c has only one box Q, including the intervals $T_\mathbf{i}$,$i = 1$,..,4, $\mathbf{Z}_c^{'}$ and H:
4. To extract from list $\mathbb{P}$ box B.
5. To calculate $m(B)$ and $M(B)$ for points C_l of the surface of the required workspace
6. If $m(B) > 0$ or $M(B) < 0$ at least for C_l, then exclude B and turn to step 9.
7. If $\left|\mathbf{Z}_c^{'}\right| < \delta$, then B add to the list $\mathbb{P}_A$ and turn to the list 9.
8. In other cases, B is divided into two equal boxes by $\mathbf{Z}_c^{'}$. Add these boxes to the end of the list$\mathbb{P}$, which is $\mathbb{P}:=\mathbb{P} \cup \{B_1\} \cup \{B_2\}$.
9. If $\mathbb{P} \neq \emptyset$, then turn to step 4.
10. To extract from the list $\mathbb{P}_A$ box B.
11. To divide B by a uniform m × m grid by dimensions and H into intervals $T_i^{(p)}$ and $H^{(p)}$, $p = 1, \ldots, m$.

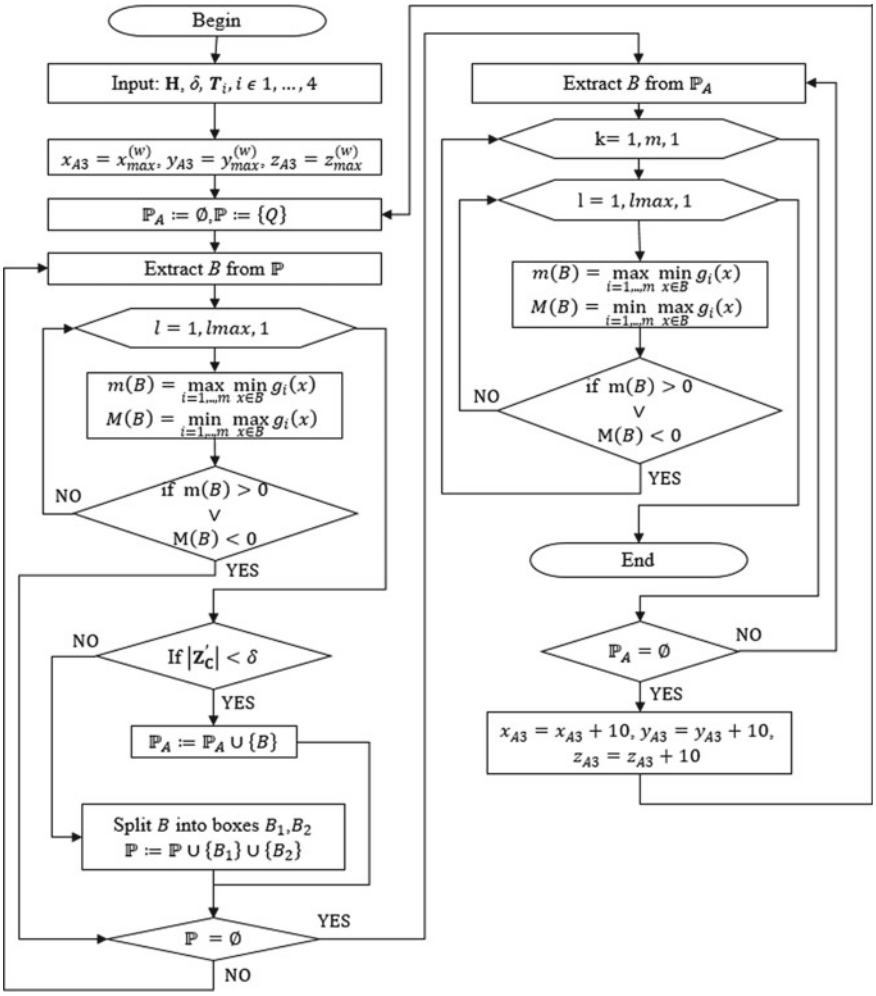

Fig. 5 Algorithm for optimization of the geometric parameters of the cable mechanism

12. To calculate $m(B)$ and $M(B)$ for the points C_l taking into account the intervals $T_i^{(p)}$ and $H^{(p)}$.
13. If $m(B) > 0$ or $M(B) < 0$ at least for one of C_l at all $T_i^{(p)}$ and $H^{(p)}$, then eliminate B and go to step 14. Otherwise, it is necessary to terminate the algorithm.
14. If $\mathbb{P}_A \neq \emptyset$, then turn to step 10.
15. Assign $x_{A3} = x_{A3} + 10$, $y_{A3} = y_{A3} + 10$, $z_{A3} + 10$ and turn to step 3.

The simulation was performed for various values of k in the range from 1.5 to 10 with interval 0.1, while $x^{(w)}_{\max} = y^{(w)}_{\max} = z^{(w)}_{\max} = 1000 \mathrm{x}^{(w)}_{\max} = \mathrm{y}^{(w)}_{\max} = \mathrm{z}^{(w)}_{\max} = 1000$ mm. Similarly, 2 configurations were considered. The simulation results for some k are given in Table 1.

Table 1 Dependence of the overall dimensions of the robot on the coefficient k

h, mm	Overall dimensions of the robot, mm*10, at the coefficient k									
	1.5	1.6	1.7	1.8	2	2.5	3	3.5	4	4.5	5
0	1473	460	334	306	265	216	192	178	168	162	157
100	1183	396	323	292	257	209	187	174	165	159	154

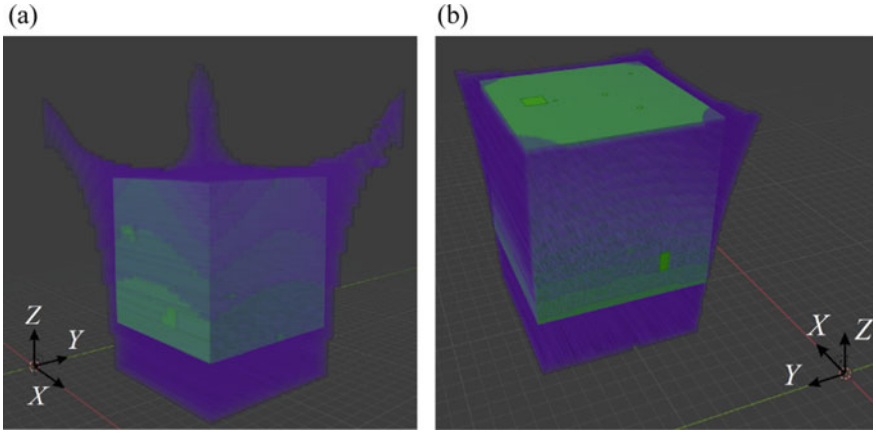

Fig. 6 Workspace for calculated overall dimensions: a) k = 3, h = 100 mm, z_{Ai} = 1870 mm, б) k = 2,5, h = 0 mm, z_{Ai} = 2160 mm

The simulation results were verified checking the entry of the 1000 × 1000 × 1000 mm cube into the workspace of the CDPR with the calculated dimensions (Fig. 6).

5 Conclusion

To conclude, we can state that for the proposed schematic and technical solution of the cable-driven parallel robot, effective numerical methods and algorithms were developed and tested, which allowed determining the minimum geometric parameters of the robot. The results showed that the configuration of the CDPR with the axial movement of the output link allows both increasing the volume of the workspace for the given overall dimensions of the robot, and reducing the overall dimensions for the required workspace during technological operations.

Acknowledgements The reported study was funded by RFBR according to the research projects 18-31-20060.

References

1. Pott, A., Mütherich, H., Kraus, W., Schmidt, V., Miermeister, P., Verl, A.: In: Pott, A., Bruckmann, T. (eds.) Cable-Driven Parallel Robots, vol. 12, pp.119–134. Springer, Berlin, Heidelberg (2013)
2. Tavolieri C., Merlet J.P., Ceccarelli, M.: A workspace analysis of a overconstrained cable-based parallel manipulator by using the interval analysis. In: 3rd International Symposium on

Multibody Systems and Mechatronics, pp. 1–13. School of Engineering, University of San Juan, Argentine (2008)
3. Gaponenko, E.V., Rybak, L.A., Kholoshevskaya, L.R.: Structural analysis and classification of robotic systems with drive mechanisms based on cable elements. Bull. BSTU Name After V.G. Shukhov. **9**, 126–136 (2019)
4. Higuchi, T., Ming, A., Jiang-Yu, J.: Application of multi-dimensional wire crane in construction. In: 5th International Symposium on Robotics in Construction, pp. 661–668. Japan Industrial Robot Association, Japan (1988)
5. Jeong, J.W., Kim, S.H., Kwak, Y.K., Smith, C.C.: Development of a parallel wire mechanism for measuring position and orientation of a robot end-effector. Mechatronics **8**, 845–861 (1998)
6. Won Jeong, J., Hyun Kim, S., Keun Kwak, Y.: Kinematics and workspace analysis of a parallel wire mechanism for measuring a robot pose. Mech. Mach. Theory **34**, 825–841 (1999)
7. Dovat, L., Lambercy, O., Gassert, R., Maeder, T., Milner, T., Leong, T.C., et al.: A cable-actuated rehabilitation system to train hand function after stroke. Neural systems and rehabilitation engineering. IEEE Trans. **16**, 582–91 (2008)
8. Ying, M., Agrawal, S.K.: Design of a cable-driven arm exoskeleton (CAREX) for neural rehabilitation Robotics. IEEE Trans. **28**, 922–931 (2012)
9. Cafolla, D., Russo, M., Carbone, G.: CUBE, a cable-driven device for limb rehabilitation. J. Bionic. Eng. **16**(3), 492–502 (2019)
10. Riechel, A., Bosscher, P., Lipkin, H., EbertUphoff, I.: Cable-driven robots for use in hazardous environments. In: 10th International Topical Meeting Robot Remote System, pp. 310–317. Hazardous Environment, Gainesville (2004)
11. Roberts, R., Graham, T., Lippitt, T.: On the inverse kinematics, statics, and fault tolerance of cable-suspended robots. J. Fielpd Robot. **15**(10), 581–597 (1998)
12. Merlet, J.P., Daney, D.A.: A portable, modular parallel wire crane for rescue operations. In: IEEE International Conference Robotics and Automation ICRA-2010, pp. 2834–2839. Institute of Electrical and Electronics Engineers Inc., USA (2010)
13. Gosselin, C.: In: Pott, A., Bruckmann, T. (eds.) Cable-Driven Parallel Robots, vol. 12, pp. 3–22. Springer, Berlin, Heidelberg (2013)
14. Duan, Q.J., Xuechao, D.: Workspace classification and quantification calculations of cable-driven parallel robots. In: Advances in Mechanical Engineering 1–9 (2014)
15. Zhang, N., Shang, W.: Dynamic trajectory planning of a 3-DOF under-constrained cable-driven parallel robot. Mech. Mach. Theory **98**, 21–35 (2016)
16. Du, J., Bao, H., Cui, C., Yang, D.: Dynamic analysis of cable-driven parallel manipulators with time-varying cable lengths. Finite Elem. Anal. Des. **48**, 1392–1399 (2012)
17. Evtushenko, Y., Posypkin, M., Rybak, L., Turkin, A.: Approximating a solution set of nonlinear inequalities. J. Global Optimization **7**, 129–145 (2018)
18. Malyshev, D.I., Posypkin, M.A., Gorchakov, AYu., Ignatov, A.D.: Parallel algorithm for approximating the workspace of a robot. Int. J. Open Informa. Technol. **7**(1), 1–7 (2019)
19. Malyshev, D., Posypkin, M., Rybak, L., Usov, A.: Approaches to the determination of the working area of parallel robots and the analysis of their geometric characteristics. Eng. Trans. **67**(3), 333–345 (2019)
20. Rybak, L.A., Gaponenko, E.V., Malyshev, D.I.: Approximation of the workspace of a cable-driven parallel robot with a movable gripper. Mech. Machine Sci. **86**, 36–43 (2020)
21. Posypkin, M., Usov, A.: Implementation and verification of global optimization benchmark problems. Open Eng. **7**(1), 470–478 (2017)